

## Evolution of structural and dynamic heterogeneities and activation energy distribution of deformation units in metallic glass

W. Jiao, P. Wen, H. L. Peng, H. Y. Bai, B. A. Sun et al.

Citation: *Appl. Phys. Lett.* **102**, 101903 (2013); doi: 10.1063/1.4795522

View online: <http://dx.doi.org/10.1063/1.4795522>

View Table of Contents: <http://apl.aip.org/resource/1/APPLAB/v102/i10>

Published by the [American Institute of Physics](http://www.aip.org).

---

### Related Articles

Compressed correlation functions and fast aging dynamics in metallic glasses

*J. Chem. Phys.* **138**, 054508 (2013)

Structural study of Al<sub>2</sub>O<sub>3</sub>-Na<sub>2</sub>O-CaO-P<sub>2</sub>O<sub>5</sub> bioactive glasses as a function of aluminium content

*J. Chem. Phys.* **138**, 034501 (2013)

Manipulating the properties of stable organic glasses using kinetic facilitation

*J. Chem. Phys.* **138**, 12A517 (2013)

Dynamics of thermal vibrational motions and stringlike jump motions in three-dimensional glass-forming liquids

*J. Chem. Phys.* **138**, 12A514 (2013)

Static correlations functions and domain walls in glass-forming liquids: The case of a sandwich geometry

*J. Chem. Phys.* **138**, 12A509 (2013)

---

### Additional information on *Appl. Phys. Lett.*

Journal Homepage: <http://apl.aip.org/>

Journal Information: [http://apl.aip.org/about/about\\_the\\_journal](http://apl.aip.org/about/about_the_journal)

Top downloads: [http://apl.aip.org/features/most\\_downloaded](http://apl.aip.org/features/most_downloaded)

Information for Authors: <http://apl.aip.org/authors>

## ADVERTISEMENT

**JANIS** Does your research require low temperatures? Contact Janis today.  
Our engineers will assist you in choosing the best system for your application.



10 mK to 800 K      LHe/LN<sub>2</sub> Cryostats  
Cryocoolers      Magnet Systems  
Dilution Refrigerator Systems  
Micro-manipulated Probe Stations

[sales@janis.com](mailto:sales@janis.com)    [www.janis.com](http://www.janis.com)  
Click to view our product web page.

## Evolution of structural and dynamic heterogeneities and activation energy distribution of deformation units in metallic glass

W. Jiao, P. Wen, H. L. Peng, H. Y. Bai, B. A. Sun, and W. H. Wang<sup>a)</sup>

*Institute of Physics, Chinese Academy of Sciences, Beijing 100190, People's Republic of China*

(Received 13 December 2012; accepted 4 March 2013; published online 13 March 2013)

We present experimental results on the distribution and evolution of energy barriers of deformation units in metallic glass (MG) via an activation-relaxation method. Our results show that the dynamical heterogeneity of metallic glass arises from its structural inhomogeneity, and there exist the close correlations between the deformation units, dynamical and structural heterogeneities, and relaxation behaviors in metallic glasses. The results might provide insights on the heterogeneities, plastic deformation, and relaxations behaviors of metallic glass. © 2013 American Institute of Physics. [<http://dx.doi.org/10.1063/1.4795522>]

The structural and dynamic heterogeneities in disordered glasses, where the topological defects are difficult to be defined, have attracted substantial interests.<sup>1–8</sup> The structural heterogeneity in the deformation model of metallic glasses (MGs) well below the glass transition temperature  $T_g$ <sup>9,10</sup> is proposed to be the “carriers” or the deformation units of the plastic flow in glass.<sup>3,5</sup> Extensive efforts have been devoted to detect the heterogeneity and to confirm the existence of the deformation units via computer simulation<sup>11,12</sup> and experimental methods.<sup>3–6,13,14</sup> However, the roles of the deformation units in the transformation from inhomogeneous to homogeneous<sup>15,16</sup> and in the homogeneous flow in apparent elastic region for prolonged time at room temperature<sup>17,18</sup> are still unclear, and their variation behaviors with temperature and time especially under deformation state are still missing.

Stress relaxation is a sensitive approach for investigating the atomic-level deformation carriers of dislocation or grain boundary in crystalline materials.<sup>19</sup> The stress relaxation was conducted in MGs to construct power dissipation maps within the supercooled liquid region<sup>20</sup> and to investigate the irreversible relaxation kinetics around  $T_g$ .<sup>21</sup> However, little work has been done on the deformation units and the dynamic heterogeneity in MGs in its nominal elastic region well below  $T_g$ . In this Letter, we apply an instantaneous activation-relaxation technique to investigate the activation energy and relaxation time spectra of the deformation units upon temperatures. Our results show that in MG, the dynamical heterogeneity arises from structural inhomogeneity, and the heterogeneities and relaxations are associated with the activation and evolution processes of the deformation units.

We used a Pd<sub>40</sub>Ni<sub>10</sub>Cu<sub>30</sub>P<sub>20</sub> MG as a model system due to its excellent glass-forming ability and high thermal stability. The Pd<sub>40</sub>Ni<sub>10</sub>Cu<sub>30</sub>P<sub>20</sub> glassy ribbon was produced by the melt-spinning method in an argon atmosphere. The tensile stress relaxation and dynamical mechanical measurement were performed on dynamic mechanical analyzer (DMA) model TA Q800. To avoid the effect of the physical aging, all the samples were previously heated up above its  $T_g$ , isothermal for 3 min, and cooled down from the supercooled

liquid state in the argon atmosphere prior to the measurements. All the stress relaxation measurements were performed on the specimens at 0.3% tensile strain for 100 min. Before the experiment, a 3 min delay was applied to allow the samples to equilibrate at the test temperature.

Figure 1(a) shows the stress response of Pd<sub>40</sub>Ni<sub>10</sub>Cu<sub>30</sub>P<sub>20</sub> MG to a constant strain of 0.3% at various temperatures well below  $T_g = 580$  K of the MG. One can see that the stress  $\sigma(t)$  shows a rapidly decrease from initial value  $\sigma_U$ , and then slows down gradually with increasing time. Ultimately, the stress approaches a saturation value  $\sigma_R$ , and the elastic strain is converted to inelastic strain gradually associated with the stress relaxation process.<sup>19</sup> The stress relaxation process is related to the activation of the deformation units similar to the creep experiments.<sup>19,22</sup> The simulations also confirm that the localized plastic deformation coincides with decreasing stress.<sup>23</sup> The increase of the test temperature leads to an increment of relaxation rate, and the relative relaxation strength of  $\Delta = (\sigma_U - \sigma_R)/\sigma_R$  for various temperatures are listed in Table I. The increase of  $\Delta$  with rising temperature indicates that more volume fraction of the MG undergoes inelastic deformation<sup>19,23</sup> and are transformed into liquid-like regions.<sup>5,6</sup> The phenomena are further confirmed via DMA shown in Fig. 1(b). In the temperature range of  $\beta$  relaxation [see Fig. 1(b)] for the stress relaxation, the storage modulus almost keeps in constant, implying that the glass state is still kept in the temperature range, whereas the associated loss factor  $\tan\delta$  increases monotonously with temperature, which corresponds to the energy loss occurring during the process<sup>24</sup> and implies that more deformation units were activated with increasing temperature.

The MG is commonly regarded to vary significantly in space due to the nature of structural heterogeneity,<sup>6</sup> which consist of loosely bonded regions acting as deformation units under deformation.<sup>5,22</sup> This implies that the energy barrier of the deformation units is also widely distributed. As the density of the thermal activation process cannot be measured directly, it can only be inferred via the detection of the property change resulting from the activation process.<sup>25</sup> Based on the activation energy spectrum model, the variation of relaxation stress  $\sigma$  on time  $t$  at  $T$  can be expressed by an integral equation<sup>25</sup>

<sup>a)</sup> Author to whom correspondence should be addressed. Electronic mail: whw@aphy.iphy.ac.cn.

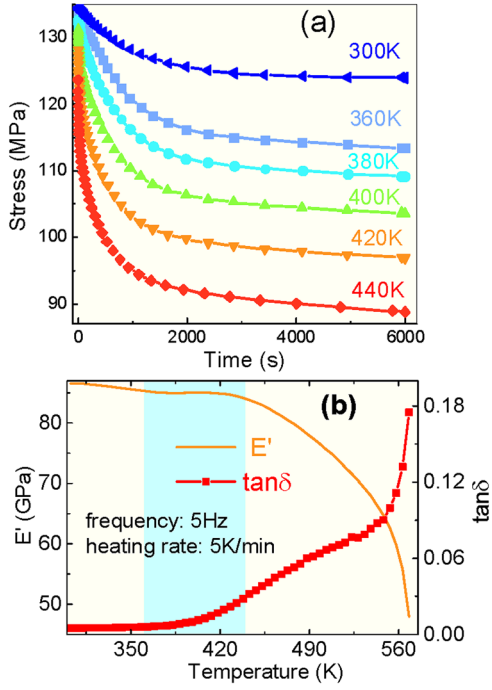


FIG. 1. (a) The stress relaxation curves of Pd<sub>40</sub>Ni<sub>10</sub>Cu<sub>30</sub>P<sub>20</sub> MG at 300, 360, 380, 400, 420, and 440 K. (b) Temperature dependence of storage modulus ( $E'$ ) and loss factor ( $\tan \delta = E'/E''$ , where  $E''$  is loss modulus) under 5 Hz and at a heating rate is 5 K/min. The shadow region represents the temperature region of  $\beta$  relaxation used for stress relaxation test.

$$\Delta\sigma(t) = \int_0^{+\infty} p(E)\theta(E, T, t)dE, \quad (1)$$

where  $p(E)$  is the total available property change induced by all the activation processes in the range of  $E$  to  $E + dE$ .  $\Delta\sigma(t) = \sigma_U - \sigma(t)$ , and  $\theta(E, T, t)$  is the characteristic annealing function:<sup>25</sup>  $\theta(E, T, t) = 1 - \exp(-t/\tau) = 1 - \exp[-v_0 t \exp(E/kT)]$ , where,  $v_0$  is an effective attack frequency of the order of the Debye frequency or less.<sup>22</sup> Assuming that during the isothermal stress relaxation at  $t$ , all processes with  $\tau < t$  contribute to the relaxation, whereas processes with  $\tau > t$  have no contribution. Correspondingly, there is a critical energy activation  $E_C$  for the deformation units, and only those units with  $E < E_C$  have the contribution to the relaxation observed on the probing time  $t$ .<sup>25</sup> In the frame of step-like approximation,<sup>3,26</sup>

$$p(E) = -\frac{1}{kT} \frac{d\sigma(t)}{d \ln t}. \quad (2)$$

TABLE I. Fitting parameters of  $\tau_m$  and  $s$  obtained from the generalized Maxwell model,  $b$  obtained from the KWW function and relaxation strength  $\Delta = (\sigma_U - \sigma_R)/\sigma_R$  of Pd<sub>40</sub>Ni<sub>10</sub>Cu<sub>30</sub>P<sub>20</sub> at different temperatures.

Temperature (K)	$\tau_m$ (S)	$s$	$\Delta$	$b$
300	1065	0.052	0.085	$1.00 \pm 0.016$
360	937	0.083	0.176	$0.982 \pm 0.014$
380	820	0.775	0.215	$0.838 \pm 0.008$
400	722	1.546	0.272	$0.647 \pm 0.01$
420	645	2.082	0.334	$0.554 \pm 0.01$
440	530	2.555	0.405	$0.483 \pm 0.006$

According to the Arrhenius equation:  $E = kT \ln(v_0 t)$ , taking  $v_0$  as the Debye frequency  $10^{-13}$ s.<sup>22</sup> The obtained apparent activation energy spectra are presented in Fig. 2(a), where  $P(E)$  is normalized by the value at the peak to highlight the relative variation of the spectra. It can be seen that the shape of the activation energy spectra is close to the Gaussian distribution and comparable to that obtained from the analysis of creep-recovery curves<sup>20</sup> and activation-relaxation simulation.<sup>27</sup> The spectra shift toward the higher value with increasing temperature, indicating that the more deformation units with higher energy barriers are activated during inelastic deformation at elevated temperature. Due to the loading rate in our case is finite, the deformation units with the characteristic activation energy smaller than  $kT \ln(v_0 \tau)$  cannot be detected, and result in only part of the activation energy spectra presented at high temperatures. As shown in Fig. 2(b), the full width at half maximum (FWHM) of the activation energy spectra also increases with temperature, implying that the statistical energy barrier distribution of the deformation units is more dispersive, and more kinds of deformation units with different activation energies are engaged into the stress relaxation process at higher temperatures. The high fraction of liquid-like deformation units with increasing temperature makes the MG more heterogeneous at higher temperatures. Reference to the result of DMA

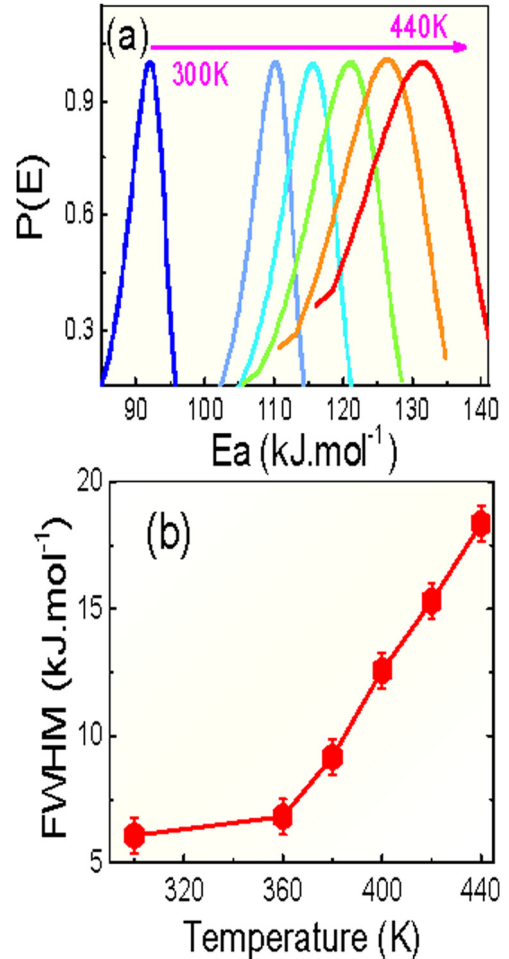


FIG. 2. (a) Temperature dependence of normalized activation energy spectra  $P(E)$  scaled by the peak value to highlight the relative variation of spectrum. (b) The variation of FWHM of activation energy spectra on temperature.

presented in Fig. 1(b), the extension of activation energy spectrum occurs slight before the activation of the  $\beta$  relaxation. However, the spectrum broadens quickly with increasing temperature associated with the operation of the  $\beta$  relaxation. This result further confirms that the  $\beta$  relaxation is closely related to the structural heterogeneity in MG.

The stress relaxation data at various temperatures can be fitted by stretched exponential function (not shown here)  $\Phi(t) = (\sigma(t) - \sigma_R) / (\sigma_U - \sigma_R) = \exp[-(t/\tau_c)^b]$ ,<sup>1</sup> where  $\tau_c$  is apparent characteristic stress relaxation time and  $b$  is a non-dimensional relaxation parameter.<sup>8,28</sup> The fitting values of  $b$  were listed in Table I. The  $b$  is almost constant before the operation of  $\beta$  relaxation implying the slight change of the deformation units. However, in the  $\beta$  relaxation temperature region, the  $b$  decreases obviously as increasing temperature, indicating that the relaxation time distribution is extended at elevated temperature, and the difference of the involved slowest and fastest deformation process becomes more obvious.<sup>8</sup> The results further confirm that the deformation units, which are closely correlated with  $\beta$  relaxation, are broadly distributed in temporal scale.

Based on the above results and the experimentally observed structural heterogeneity of MG,<sup>5,22</sup> the relaxation time of these deformation units in MG can be considered to have a broad distribution. Figure 3(a) schematically shows each deformation unit  $i$  signed by the relaxation time  $\tau_i$  and confined by the surrounding elastic matrix in MG. When the applied strain is much lower than the yield strain, the deformation units are in the state of “dilute solution” and do not interact with each other.<sup>22</sup> Thus, the generalized Maxwell model (linear solid model) can be applied to analyze the stress relaxation behavior of MG<sup>29,30</sup> as presented in Fig. 3(b). The deformed unit is represented by dashpot, and the

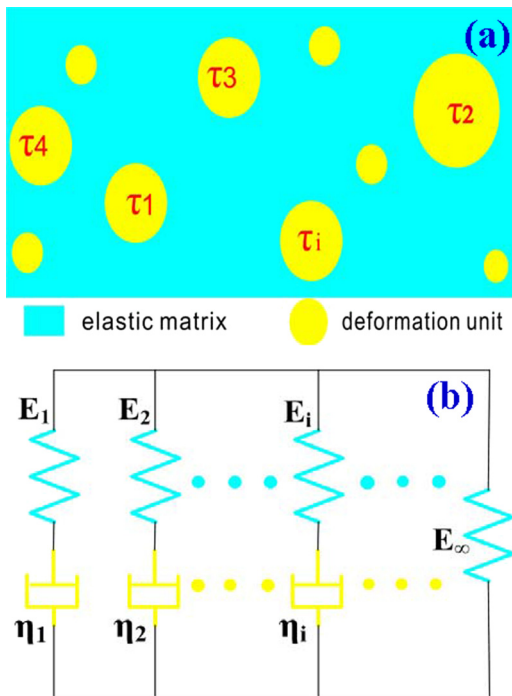


FIG. 3. (a) The schematic illustration of MG composed of elastic matrix and patched deformation units. (b) Generalized Maxwell model: relaxation processes in parallel, where  $i$ -type site are associated with modulus  $E_i$ , viscosity  $\eta_i$ , and relaxation time  $\tau_i = \eta_i/E_i$ .

glassy matrix deforms elastically is represented by spring. The  $\tau_i$  is then determined by the  $i$ th Maxwell unit consisting of a spring  $E_i$  and a dashpot  $\eta_i$  in series. In the stress relaxation, each Maxwell element is subjected to an instantaneous strain  $\varepsilon_0$ , which is the sum of elastic and inelastic strains and kept constant all the time.<sup>19</sup> So that

$$\frac{1}{E_i} \frac{d\sigma_i}{dt} + \frac{\sigma_i}{\eta_i} = 0. \quad (3)$$

As shown in Fig. 3(b),  $N$  Maxwell units and one spring are connected in parallel, this leads to:  $\sigma(t) = \varepsilon_0 E_\infty + \varepsilon_0 \sum_{i=1}^N E_i e^{-t/\tau_i}$ , where  $\tau_i = \eta_i/E_i$ . Due to the intrinsic random nature of the amorphous samples,<sup>3,22</sup> we assume a continuum spectrum of relaxation times. Thus, the time dependence of  $\sigma(t)$  is<sup>29,30</sup>

$$\sigma(t) = \sigma_R + \int_{-\infty}^{+\infty} H(\ln\tau) e^{-t/\tau} d \ln \tau, \quad (4)$$

where the  $H(\ln\tau)$  is the logarithm distribution function of  $\tau$ . Considering the facts that the activation energy spectrum and the broad distribution of elastic constants in MGs are close to the Gaussian distribution and  $\tau = \tau_0 \exp(E_a/KT)$ ,<sup>6</sup> we speculate that the  $\tau$  of deformation units satisfies the lognormal distribution:  $H(\ln\tau) = k \exp(-\frac{(\ln\tau - \ln\tau_m)^2}{s^2})$ , where  $\tau_m$  is the most probable relaxation time,  $s$  is the width of the  $\tau$  spectrum, and  $k$  is the factor in front of exponential. As shown in Fig. 4(a), the representative result of stress relaxation data at 380 K can be well simulated by the generalized

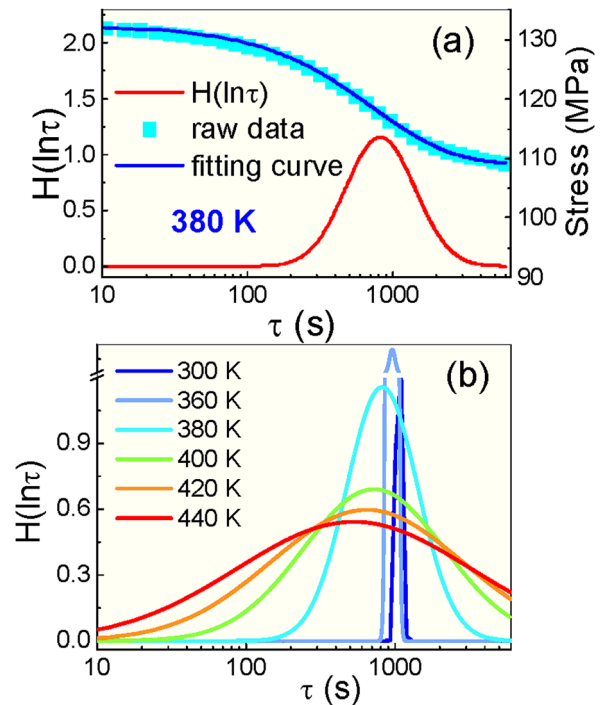


FIG. 4. (a) The stress relaxation data at a representative temperature of 380 K was fitted by the generalized Maxwell model, and the corresponding continuous  $\tau$  spectrum was obtained. (b) Continuous relaxation time spectra at 300, 360, 380, 400, 420, and 440 K computed analytically from the fitting.

Maxwell model, and the associated relaxation time spectrum at 380 K is also obtained and shown in Fig. 4(a). The  $\tau$  spectrum spans several orders of magnitude implying that the deformation units are broadly distributed in temporal scale and the dynamics of the stress relaxation are strongly heterogeneous, and the dynamical heterogeneity appears to arise from the structural inhomogeneity. The relaxation time spectra at various temperatures were also obtained and shown in Fig. 4(b), and the fitting parameters of  $\tau_m$  and  $s$  are listed in Table I. It is shown that the  $\tau_m$  decreases with temperature, implying the relaxation rate is accelerated at elevated temperature. The  $\tau$  distribution presented in Fig. 4(b) not only shifts leftward but also becomes broader. This indicates that the increase of temperature results in the activation of more deformation units.<sup>31</sup> The additional activated deformation units at higher temperature lead to the expansion of relaxation time spectrum, suggesting that the higher the temperature, the more dispersive the relaxation time distribution, the stronger the heterogeneity, especially in  $\beta$  relaxation region. Because the sampling time range is finite, the relaxation time spectra at low temperatures can show almost full configuration, whereas at high temperature, only part of that were presented.

The main implication of the attained activation energy and relaxation time spectra is that the activation of the deformation units are not uniform, but are operated gradually with time. Only the units whose relaxation times are shorter than the observation time have contribution to the inelastic deformation. The results also indicate that the dynamical heterogeneity might arise from structural inhomogeneity due to the variation of atomic mobility in densely and loosely packed regions.<sup>4,32</sup> The inhomogeneity may be the origin of anelastic deformation in apparent elastic region and responsible for the transition from anelasticity to viscoelasticity in MGs at room temperature.<sup>17,18</sup> The deformation units with low energy barriers and short relaxation time are activated gradually in nominal elastic range by thermal energy or external stress at enough long time, and then lead to viscoelastic response once the fraction of the deformation units comes to the percolation limit.<sup>6</sup>

The results are helpful for understanding the inhomogeneous to homogeneous transition of MG in the deformation map.<sup>15</sup> The MG deforms inhomogeneously for  $T < 0.8T_g$ ,<sup>5</sup> and the fraction of liquid-like zone increases with temperature as more deformation units activated. This is backed up by apparent activation volume calculation,<sup>33</sup> which show that the size of the average deformation units increases from approximately 0.2 nm<sup>3</sup> at 77 K to about 2.0 nm<sup>3</sup> at 195 K. Further increasing temperature, more deformation units are activated, and the MG then is composed of a patchwork of solid-like domains separated by “soft” regions walls, and the homogeneous deformation then occurs.<sup>34</sup> During this transition process, there might be a critical point corresponding to the percolation of liquid-like zone, which is associated with the strongest heterogeneous state.<sup>35</sup> In the test temperature range, the higher the temperature, the more dispersive the spectrum, the stronger the heterogeneity, and the more pronounced the  $\beta$  relaxation. This confirms that the  $\beta$  relaxation is closely related to the heterogeneity in MG.

Our observations suggest a plausible picture regarding structural heterogeneity, the dynamic relaxations, and plasticity in MG, which can provide information for tough MGs design: The broad activation energy distribution is the indicator of abundant potential deformation units with lower activation energies in the system, and global plasticity can then be triggered as long as the fraction of the activated deformation units reaches the percolation limit by external stresses.

Insightful discussion with A. Lemaitre and Q. P. Kong are appreciated. This work was supported by MOST 973 of China (No. 2010CB731603) and the NSF of China (51271195 and 51071170).

<sup>1</sup>M. D. Ediger and P. Harrowell, *J. Chem. Phys.* **137**, 080901 (2012).

<sup>2</sup>P. G. Debenedetti and F. H. Stillinger, *Nature* **410**, 259 (2001).

<sup>3</sup>W. Dmowski, T. Iwashita, C. P. Chuang, J. Almer, and T. Egami, *Phys. Rev. Lett.* **105**, 205502 (2010).

<sup>4</sup>Y. H. Liu, D. Wang, K. Nakajima, W. Zhang, A. Hirata, T. Nishi, A. Inoue, and M. W. Chen, *Phys. Rev. Lett.* **106**, 125504 (2011).

<sup>5</sup>J. C. Ye, J. Lu, C. T. Liu, Q. Wang, and Y. Yang, *Nature Mater.* **9**, 619 (2010).

<sup>6</sup>H. Wagner, D. Bedorf, S. Kuechemann, M. Schwabe, B. Zhang, W. Arnold, and K. Samwer, *Nature Mater.* **10**, 439 (2011).

<sup>7</sup>B. Yang, C. T. Liu, T. G. Nieh, M. L. Morrison, P. K. Liaw, and R. A. Buchanan, *J. Mater. Res.* **21**, 915 (2006).

<sup>8</sup>L. Berthier, *Dynamical Heterogeneities in Glasses, Colloids and Granular Media* (Oxford University Press, Oxford, 2011).

<sup>9</sup>A. S. Argon, *Acta Metall.* **27**, 47 (1979).

<sup>10</sup>M. L. Falk and J. S. Langer, *Phys. Rev. E* **57**, 7192 (1998).

<sup>11</sup>H. L. Peng, M. Z. Li, and W. H. Wang, *Phys. Rev. Lett.* **106**, 135503 (2011).

<sup>12</sup>F. Delogu, *Phys. Rev. Lett.* **100**, 255901 (2008).

<sup>13</sup>T. Ichitsubo, H. S. Chen, and J. Saida, *Phys. Rev. Lett.* **95**, 245501 (2005).

<sup>14</sup>Y. Wu and Z. P. Lu, *J. Appl. Phys.* **106**, 083512 (2009).

<sup>15</sup>P. Schall and F. Spaepen, *Science* **318**, 1895 (2007).

<sup>16</sup>H. B. Yu, L. Gu, W. H. Wang, and H. Y. Bai, *Phys. Rev. Lett.* **108**, 015504 (2012).

<sup>17</sup>K. W. Park, C. M. Lee, M. L. Falk, and J. C. Lee, *Acta Mater.* **56**, 5440 (2008).

<sup>18</sup>H. B. Ke, P. Wen, W. H. Wang, and A. L. Greer, *Scr. Mater.* **64**, 966 (2011).

<sup>19</sup>T. T. Lau, A. Kushima, and S. Yip, *Phys. Rev. Lett.* **104**, 175501 (2010).

<sup>20</sup>K. S. Lee, J. Eckert, and Y. W. Chang, *J. Non-Cryst. Solids* **353**, 2515 (2007).

<sup>21</sup>O. P. Bobrov, S. N. Laptev, and V. A. Khonik, *Phys. Solid State* **46**, 470 (2004).

<sup>22</sup>A. S. Argon and H. Y. Kuo, *J. Non-Cryst. Solids* **37**, 241 (1980).

<sup>23</sup>M. Neudecker and S. G. Mayr, *Acta Mater.* **57**, 1437 (2009).

<sup>24</sup>Z. F. Zhao, P. Wen, C. H. Shek, and W. H. Wang, *Phys. Rev. B* **75**, 174201 (2007).

<sup>25</sup>M. R. J. Gibbs, J. E. Evetts, and J. A. Leake, *J. Mater. Sci.* **18**, 278 (1983).

<sup>26</sup>S. V. Khonik, A. Pompe, and V. A. Khonik, *Phys. Rev. Lett.* **100**, 065501 (2008).

<sup>27</sup>D. Rodney and C. Schuh, *Phys. Rev. Lett.* **102**, 235503 (2009).

<sup>28</sup>B. Ruta, Y. Chushkin, G. Monaco, L. Cipelletti, E. Pineda, P. Bruna, V. M. Giordano, and M. Gonzalez-Silveira, *Phys. Rev. Lett.* **109**, 165701 (2012).

<sup>29</sup>A. S. Nowick and B. S. Berry, *Anelastic Relaxation in Crystalline Solids* (Academic Press, New York, 1972).

<sup>30</sup>J. D. Ferry, *Viscoelastic Properties of Polymers* (Wiley, New York, 1961).

<sup>31</sup>J. D. Ju, D. Jang, A. Nwankpa, and M. Atzmon, *J. Appl. Phys.* **109**, 053522 (2011).

<sup>32</sup>F. Delogu, *Phys. Rev. B* **79**, 184109 (2009).

<sup>33</sup>A. Dubach, F. H. Dalla Torre, and J. F. Loeffler, *Philos Mag. Lett.* **87**, 695 (2007).

<sup>34</sup>E. V. Russell and N. E. Israeloff, *Nature* **408**, 695 (2000).

<sup>35</sup>J. S. Harmon, M. D. Demetriou, W. L. Johnson, and K. Samwer, *Phys. Rev. Lett.* **99**, 135502 (2007).